WALAILAK JOURNAL
http://wjst.wu.ac.th Engineering and Physical Sciences

Chemically Reacting MHD Dusty Nanofluid Flow over a Vertical Cone with Non-Uniform Heat Source/Sink

Janke Venkata RAMANA REDDY[1], Vanagala SUGUNAMMA[1,*], Naramgari SANDEEP[2] and Chakravarthula SK RAJU[2]

[1]*Department of Mathematics, S.V. University, Tirupati-517502, India*
[2]*Division of Fluid Dynamics, VIT University, Vellore-632014, India*

([*]Corresponding author's e-mail: vsugunar@gmail.com)

Received: 12 August 2015, Revised: 1 January 2016, Accepted: 18 February 2016

Abstract

This paper comprehensively analyzes the momentum, heat and mass transfer behavior of a chemically reacting magnetohydrodynamic (MHD) nanofluid flow embedded with conducting dust particles past a cone in the presence of non-uniform heat source/sink, volume fractions of dust, and nanoparticles. We consider Cu-water and Al_2O_3-water nanofluids embedded with conducting dust particles for this study. The governing partial differential equations of the flow, heat, and mass transfer are transformed into nonlinear ordinary differential equations by using self similarity transformations, which are further solved numerically using the Runge-Kutta based Newton's method. The effects of various non-dimensional governing parameters on velocity, temperature, and concentration profiles are discussed with the help of graphs. Furthermore, the effects of these parameters on skin friction coefficient, Nusselt numbers, and Sherwood numbers are also discussed and presented through tables. Moreover, it is found that an increase in the mass concentration of dust particles depreciates the velocity profiles of fluid and dust phases. It is also found that an increase in fluid particle interaction enhances the thermal conductivity of the flow.

Keywords: MHD, dusty fluid, nanofluid, vertical cone, non-uniform heat source/sink

Nomenclatures:

x	dimensional distance along the surface of the cone
y	dimensional distance normal to the surface of the cone
u, v	dimensional velocity components of nanofluid along $x, y-$ axis directions respectively
u_p, v_p	dimensional velocity components of dust phase along $x, y-$ axis directions respectively
r	local radius of the cone
B_0	strength of the external magnetic field
T, C	temperature and concentration of the fluid respectively
T_w, C_w	temperature and concentration distributions along the surface of the cone respectively
T_∞, C_∞	ambient temperature and concentration respectively
K	Stoke's resistance
N	number density of dust particles
m	mass of the dust particles
ρC_P	heat capacitance
k_{nf}	thermal conductivity
N_1	density of the dust particles phase
D_m	molecular diffusivity
k_0	dimensioned chemical reaction parameter

Gr	Grashof number
g	acceleration due to gravity
A^*, B^*	space and temperature dependent internal heat generation/absorption parameters
f', F'	dimensionless velocities of fluid phase and dust phase respectively
M	magnetic field parameter
λ	buoyancy ratio
Pr	Prandtl number
Ec	Eckert number
Sc	Schmidt number
Kr	dimensionless chemical reaction parameter

Greek symbols:

τ_υ	relaxation time of the dust particle
σ	electrical conductivity
ρ	density
ϕ	volume fraction of nanoparticles
ϕ_d	volume fraction of dust particles
μ	dynamic viscosity
υ	kinematic viscosity
β	coefficient of thermal expansion due to temperature differences
β^*	coefficient of thermal expansion due to concentration differences
γ	half angle of the cone
η	similarity variable
θ	dimensionless temperature
ψ	dimensionless concentration
α	mass concentration of the dust particles
β	fluid particle interaction parameter

Subscripts:

nf	nanofluid
f	base fluid
s	solid nanoparticles

Introduction

The suspension of nano sized metallic or non-metallic particles in base fluids gives nanofluid. The metals can be Cu, Hg, Ag, etc., and the non-metals can be Al_2O_3, TiO_2, etc. Generally, base fluids like water, kerosene, and ethylene glycol have low thermal conductivity, but the suspension of the above mentioned metals or non-metals in nano size (1 - 100 nm) form helps to enhance the thermal conductivity of the base fluids. Several researchers investigated the characteristics of nanofluids and found that the thermal conductivity of base fluids can be improved by the inclusion of nanoparticles.

Masuda *et al*. [1] observed an enhancement in the thermal conductivity of the base fluid by the dispersion of ultra-fine particles in the base fluids. Further, Liu *et al*. [2] proved that there is an enhancement in the thermal conductivity with carbon nanofluids, and Yu *et al*. [3] proved this result by considering kerosene based Fe_3O_4 nanofluids. Especially over the past few years, the research on nanofluids has been very much improved due to its various industrial applications in electronic cooling systems and radiators. Therefore, researchers like Beck *et al*. [4], Awad *et al*. [5], and Raju *et al*. [6] have found the effects of different physical parameters on the flow of nanofluids over different channels with the help of their investigations.

Research on dusty fluids also proved that an inclusion of micrometer sized dust particles to base fluids helps to improve thermal conductivity. In addition to this, dusty fluids have a wide range of industrial applications, as well as in science and technology. Due to these facts, several researchers investigated the flow characteristics of dusty fluids. Among them, Ramana Reddy *et al*. [7] analyzed the heat generation or absorption effects on dusty viscous flow under the influence of aligned magnetic field. Gireesha *et al.* [8] discussed the magnetohydrodynamic (MHD) heat transfer effects on dusty fluid flow over a stretching sheet. The combined heat and mass transfer flow along with MHD effects have tremendous applications in power transformer electronics solar energy systems, etc. Owing to this fact, Sandeep and Sugunamma [9] discussed the radiation effects on the flow past a vertical plate under the influence of inclined magnetic field. Seth *et al*. [10] analyzed the effects of heat and mass transfer on the flow past an accelerated moving vertical plate.

Mohan Krishna *et al*. [11] analyzed the influence of radiation and chemical reaction on MHD convective flow with suction and heat generation effects. Abu Bakar *et al*. [12] reported the MHD

boundary layer flow of a Maxwell nanofluid in a vertical surface with suction or injection effects. In this study, they found that suction parameters have tendency to increase the velocity profiles of the flow. The flow of viscous Ag-water and Cu-water nanofluids past a stretching surface was analyzed by Vajravelu *et al*. [13]. On the other hand, the flow of Jeffrey fluid with nanoparticles was analyzed by Hayat *et al*. [14]. In recent years, all the researchers of fluid dynamics have concentrated their work on the flow of different types of fluids, like Eyring Powell fluid, Maxwell fluid, Oldroid B-fluid etc. However, due to the improvement of nanotechnology, in addition to the ample applications of nanofluids, it is necessary to analyze the transfer characteristics of dusty nanofluids. To understand the mechanism of convective heat transfer, it is important to study the flow behavior past axisymmetric structures, such as vertical and horizontal cylinders, cone and spheres etc. Therefore, Roy *et al*. [15], Ravindran *et al*. [16], and Khan and Sultan [17] concentrated their research on the flow behavior of the fluids through different channels. Awais *et al*. [18] discussed the boundary layer flow of Maxwell nanofluid. Further, Hayat *et al*. [19] analyzed the influence of radiation on the flow of an Oldroid-B fluid with nanoparticles. Nadeem and Saleem [20] discussed the unsteady Eyring Powell nanofluid flow in a rotating cone. Recently, the influence of buoyancy ratio thermophoresis parameters on the transient boundary layer flow of a nanofluid over a vertical cone was analyzed by Vasu and Manish [21]. With the help of this study, they found that increase in buoyancy ratio parameter slows down the motion of the fluid. Ramesh [22] discussed the stagnation point flow of a Jeffery nanofluid towards a stretching surface. Since both the nanofluids and dusty fluids are useful in enhancing thermal conductivity, Gorla et *al.* [23] investigated the MHD flow of a dusty nanofluid over an exponentially stretching sheet with non-uniform source/sink effects. Through this study, they concluded that increase in heat source parameter causes enhancement in both base fluid and temperature profiles. Sandeep and Sulochana [24] studied the MHD flow of dusty nanofluids over a stretching surface. This study concluded that an increase in the volume fraction of dust particles reduces the velocity, but enhances the temperature profiles.

Still, no attempt has been made by the past researchers to analyze the flow, heat, and mass transfer behavior of MHD dusty nanofluids past a cone. So, by making use of all the above cited articles, we here attempt to analyze the heat and mass transfer in MHD dusty nanofluids past a cone under the influence of non-uniform heat source/sink along with the volume fractions of nano and dust particles. The reduced governing equations of the flow are solved numerically. Further, the effects of various physical parameters involved in the governing equations are discussed through graphs, which are drawn with the help of the MATLAB package. Also, the influence of different parameters on skin friction, Nusselt numbers, and Sherwood numbers are presented through tables.

Materials and methods

Mathematical analysis

Consider a steady, laminar, incompressible boundary layer flow of a dusty nanofluid over a vertical cone pointing downward with half angle γ and radius r. The *x*-axis varies along the surface of the cone and the y-axis is normal to the surface of the cone, as shown in **Figure 1**. The origin is located at the vertex of the cone. The flow field is exposed by the influence of external magnetic field strength B_0 along the *x*-axis. Both the temperature distribution T_w and concentration distribution C_w will vary along the surface of the cone. Buoyancy forces will arise due to the variations in temperature, as well as concentration in the fluid. The fluid has a uniform ambient temperature T_∞ and an ambient concentration C_∞. Here in this study, both the fluid and dust particles are assumed to be static at the beginning. The dust particles are assumed to be conducting and uniform in size. Spherical shaped nano and dust particles are considered. Number density of the dust particles, along with volume fraction, is taken into consideration. Also, the number density of the dust particles is assumed to be constant throughout the flow. It is also assumed that the external electrical field due to polarization is negligible. The drag force is taken into account for the fluid and dust particles interaction. The Boundary layer equations, which

govern the flow of the present problem according to the assumptions made above, are given, per Sandeep and Sulochana [24], by;

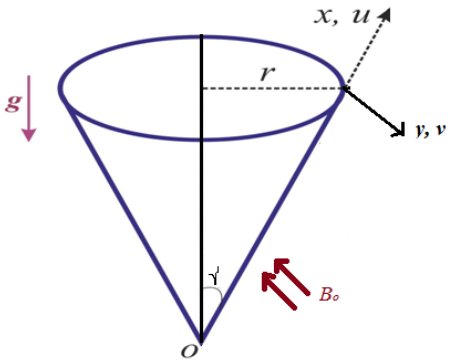

Figure 1 Geometrical representation of the problem.

$$\frac{\partial(ru)}{\partial x}+\frac{\partial(rv)}{\partial y}=0, \tag{1}$$

$$\frac{\partial(ru_p)}{\partial x}+\frac{\partial(rv_p)}{\partial y}=0, \tag{2}$$

$$\rho_{nf}(1-\phi_d)\left(u\frac{\partial u}{\partial x}+v\frac{\partial u}{\partial y}\right)=(1-\phi_d)\left[\mu_{nf}\frac{\partial^2 u}{\partial y^2}+g(\rho\beta)_{nf}(T-T_\infty)\cos\gamma+g(\rho\beta^*)_{nf}(\mathrm{C}-C_\infty)\cos\gamma\right]+$$
$$KN(u_p-u)-\sigma B^2 u, \tag{3}$$

$$Nm\left(u_p\frac{\partial u_p}{\partial x}+v_p\frac{\partial u_p}{\partial y}\right)=KN(u-u_p), \tag{4}$$

$$(\rho c_p)_{nf}\left(u\frac{\partial T}{\partial x}+v\frac{\partial T}{\partial y}\right)=k_{nf}\frac{\partial^2 T}{\partial y^2}+\frac{N_1}{\tau_\upsilon}(u_p-u)^2+q''', \tag{5}$$

$$u\frac{\partial C}{\partial x}+v\frac{\partial C}{\partial y}=D_m\frac{\partial^2 C}{\partial y^2}-k_o(C-C_\infty), \tag{6}$$

The appropriate boundary conditions of the problem are given, per Khan and Sultan [17], by;

$$\left.\begin{aligned} &u=U_w(x)=\frac{\upsilon_f}{x}(Gr)^{\frac{1}{2}},\ v=0, T=T_w(x)=ax, C=C_w(x)=ax \quad at\ \ y=0,\\ &u\to 0, u_p\to 0, v_p\to v, T\to T_\infty, C\to C_\infty \qquad\qquad as\ \ y\to\infty, \end{aligned}\right\} \tag{7}$$

where u,v are the velocities of the nanofluid along the x and y directions, respectively. Similarly, u_p, v_p stands for the velocities of dust phase along the x and $y-$ directions, respectively. $r=x\sin\gamma$ is the local radius of the cone, a is the constant, ϕ_d is the volume fraction of the dust particles, g is the acceleration

due to gravity, ρ_{nf} is the density of the nanofluid, β_{nf} is the coefficient of thermal expansion of the nanofluid due to temperature difference, β^*_{nf} is the coefficient of thermal expansion of the nanofluid due to concentration difference, T and C are the temperature and the concentration of the fluid, T_w and C_w are the temperature and the concentration of the fluid far away from the surface of the cone, T_∞ and C_∞ are the ambient temperature and the concentration of the fluid, respectively, K is the Stoke's resistance, N is the number density of dust particles, σ is the electrical conductivity of the fluid, m is the mass of the dust particle, $(\rho C_P)_{nf}$ is the heat capacitance of the nanofluid, k_{nf} is the thermal conductivity of the nanofluid, $N_1 = Nm$ is the density of the particle phase, τ_υ is the relaxation time of the dust particle, D_m is the molecular diffusivity, and k_0 is the dimensioned chemical reaction parameter.

The space and temperature dependent heat generation/absorption (non-uniform heat source/sink) q''' is defined per Dulal pal [25] by;

$$q''' = \left(\frac{k_f U_w(x,t)}{x\upsilon_f}\right)\left(A^*(T_w - T_\infty)f' + B^*(T - T_\infty)\right), \tag{8}$$

Here, A^* and B^* are parameters of the space and temperature dependent internal heat generation/absorption. The positive and negative values of A^* and B^* represents heat generation and absorption respectively. The nanofluid constants are given, per Das [26], by;

$$\left.\begin{aligned} &(\rho\beta)_{nf} = (1-\phi)(\rho\beta)_f + \phi(\rho\beta)_s, \quad (\rho c_p)_{nf} = (1-\phi)(\rho c_p)_f + \phi(\rho c_p)_s, \\ &\frac{k_{nf}}{k_f} = \frac{(k_s + 2k_f) - 2\phi(k_f - k_s)}{(k_s + 2k_f) + \phi(k_f - k_s)}, \ \mu_{nf} = \frac{\mu_f}{(1-\phi)^{2.5}}, \rho_{nf} = (1-\phi)\rho_f + \phi\rho_s, \end{aligned}\right\} \tag{9}$$

where ϕ is the volume fraction of the nanoparticles. The subscripts nf, f ,and S refer to nanofluid, base fluid, and solid properties, respectively.

Now, we introduce the following similarity transformations to make the governing Eqs. (1) - (6) into coupled nonlinear ordinary differential equations, subject to the boundary conditions given in Eq. (7).

$$\left.\begin{aligned} &u = \frac{\upsilon_f}{x}(Gr)^{\frac{1}{2}} f'(\eta), v = \frac{\upsilon_f}{x}(Gr)^{\frac{1}{4}}\left(\frac{\eta}{4}f'(\eta) - \frac{1}{2}f(\eta)\right), \eta = \frac{y}{x}(Gr)^{\frac{1}{4}}, \\ &u_p = \frac{\upsilon_f}{x}(Gr)^{\frac{1}{2}} F'(\eta), v_p = \frac{\upsilon_f}{x}(Gr)^{\frac{1}{4}}\left(\frac{\eta}{4}F'(\eta) - \frac{1}{2}F(\eta)\right), \\ &\theta(\eta) = \frac{T - T_\infty}{T_w - T_\infty}, \psi(\eta) = \frac{C - C_\infty}{C_w - C_\infty}, Gr = \frac{\rho g x^3 \cos\gamma\left(T_w - T_\infty\right)}{\upsilon_f^2}, \end{aligned}\right\} \tag{10}$$

Now, we define the dimensionless stream function by

$ru = \dfrac{\partial\Psi}{\partial y}$ and $rv = -\dfrac{\partial\Psi}{\partial x}$, where $\Psi = vx\sin\gamma(Gr)^{\frac{1}{4}} f(\eta)$.

Using the Eqs. (8) - (10) in Eqs. (3) - (7) results in the following Eqs. (11) - (14). Eq. (1) and (2) identically satisfies.

$$f'''-(1-\phi)^{2.5}\left(1-\phi+\phi(\rho_s/\rho_f)\right)\left(\frac{f'^2}{2}-\frac{ff''}{2}\right)+\left(1-\phi+\phi\left((\rho\beta)_s/(\rho\beta)_f\right)\right)\theta+$$
$$\left(1-\phi+\phi\left((\rho\beta^*)_s/(\rho\beta^*)_f\right)\right)\lambda\psi+\frac{(1-\phi)^{2.5}}{(1-\phi_d)}\left(\Lambda\alpha\beta\left(f'-F'\right)-Mf'\right)=0, \tag{11}$$

$$\left(\frac{F'^2}{2}-\frac{FF''}{2}\right)-\beta\left(f'-F'\right)=0, \tag{12}$$

$$\frac{1}{\Pr}\frac{1}{\left(1-\phi+\phi\left((\rho c_p)_s/(\rho c_p)_f\right)\right)}\left[\frac{k_{nf}}{k_f}\theta''+\Pr\alpha\beta Ec(F'-f')^2+(A^*f'+B^*\theta)\right]+\frac{1}{2}f\theta'=0, \tag{13}$$

$$\frac{1}{Sc}\psi''+\frac{1}{2}f\psi'-Kr\psi=0, \tag{14}$$

Subject to boundary conditions;

$$\left.\begin{aligned} &f(\eta)=S, f'(\eta)=1, \theta(\eta)=1, \psi(\eta)=1 && at\ \eta=0,\\ &f'(\eta)=0, F'(\eta)=0, F(\eta)=f(\eta), \theta(\eta)=0, \psi(\eta)=0 && as\ \eta\to\infty, \end{aligned}\right\} \tag{15}$$

where $\alpha=\frac{Nm}{\rho_f}$ is the mass concentration of the dust particles, $\Lambda=\frac{x^2\,\mathrm{Re}}{\upsilon_f Gr}$ is the fluid parameter, $\beta=\frac{1}{\tau_v}$ is the fluid particle interaction parameter for the velocity with $\tau_v=\frac{m}{K}$, $M=\frac{\sigma B_0^2 x^2}{\rho_f\upsilon_f(Gr)^{\frac{1}{2}}}$ is the magnetic field parameter, $\lambda=\frac{(\beta^*)_f(C_w-C_\infty)}{(\beta)_f(T_w-T_\infty)}$ is the buoyancy ratio, $\Pr=\frac{\upsilon_f}{k_f}$ is the Prandtl number, $Ec=\frac{\upsilon_f(Gr)^{\frac{1}{2}}}{(C_p)_f}$ is the Eckert number, A^* and B^* are the heat source/sink parameters, $Sc=\frac{\upsilon_f}{D_m}$ is the Schmidt number, and $Kr=\frac{k_0x^2}{\upsilon_f(Gr)^{\frac{1}{2}}}$ is the chemical reaction parameter.

Approaching this from an engineering application point of view, the local skin friction coefficient C_f, local Nusselt number Nu_x, and local Sherwood number Sh_x are given by

$$C_f\,\mathrm{Re}_x^{1/2}=f''(0), Nu_x\,\mathrm{Re}_x^{-1/2}=-\theta'(0), Sh_x\,\mathrm{Re}_x^{-1/2}=-\psi'(0), \tag{16}$$

Results and discussion

In order to solve the coupled nonlinear ordinary differential Eqs. (11) - (14) with the help of the boundary conditions of the flow represented by Eq. (15), we make use of the Runge-Kutta based Newton's method presented by Mallikarjuna *et al*. [27]. Further, the effects of various parameters on velocity, temperature, and concentration distribution involved in the Eqs. (11) - (14) are studied through graphs. For numerical results, we consider $M = 1, \phi_d = 0.1,\ \lambda = 1,\ \alpha = 0.2,\ \beta = 0.5,\ \mathrm{Pr} = 0.72,\ Ec = 0.8,$ $\phi = 1,\ A^* = 1,\ B^* = 1,\ kr = 0.5$, and $Sc = 0.66$. These values have been kept in common for the entire study, except the varied values as displayed in the respective figures and tables. The thermo physical properties of H_2O, Cu and Al_2O_3 are taken as in **Table 1**.

Table 1 Thermo physical properties of water, Cu and Al_2O_3 nanoparticles.

	ρ $(Kg\,m^{-3})$	c_p $(J\,Kg^{-1}\,K^{-1})$	k $(W\,m^{-1}\,K^{-1})$	β $(10^{-5}\,K^{-1})$
H_2O	997.1	4179	0.613	21
Cu	8933	385	401	1.67
Al_2O_3	3970	765	46	0.63

The influence of magnetic field parameter M can be seen in **Figure 2**. It is observed that an increase in the magnetic field parameter reduces the velocity profiles of both the fluid and dust phases. This is due to the fact that an increase in the magnetic field parameter develops an opposite force to the flow, called the Lorentz force. This force has the tendency to slow down the motion of the fluid in the boundary layer. Hence, it leads to enhanced deceleration of the flow.

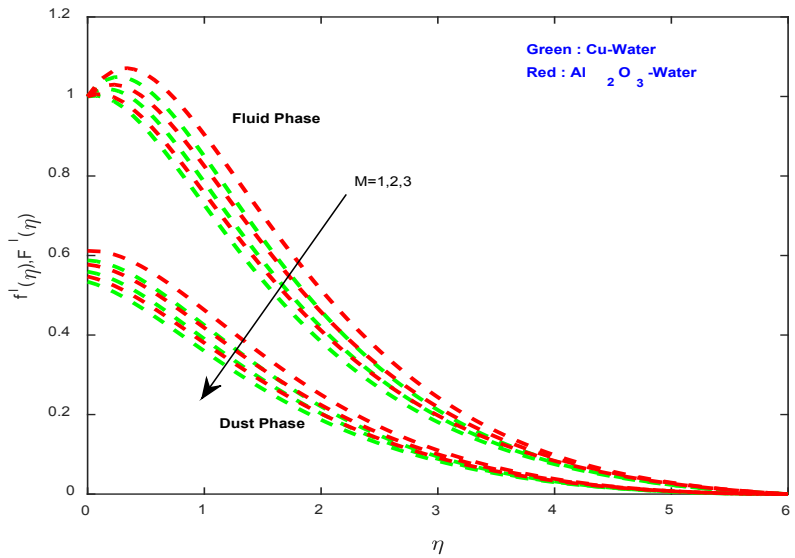

Figure 2 Velocity profiles for different values of magnetic field parameter M.

Figures 3 and **4** illustrate the effect of volume fraction of nanoparticles ϕ on velocity and temperature profiles, respectively. It is observed that an increase in the volume fraction of the nanoparticles helps to improve the velocity of the fluid as well as the dust phases over the boundary layer of the cone, but the reverse action takes place in temperature profiles, due to the fact that improvement in the velocity profiles enhances the thermal conductivity.

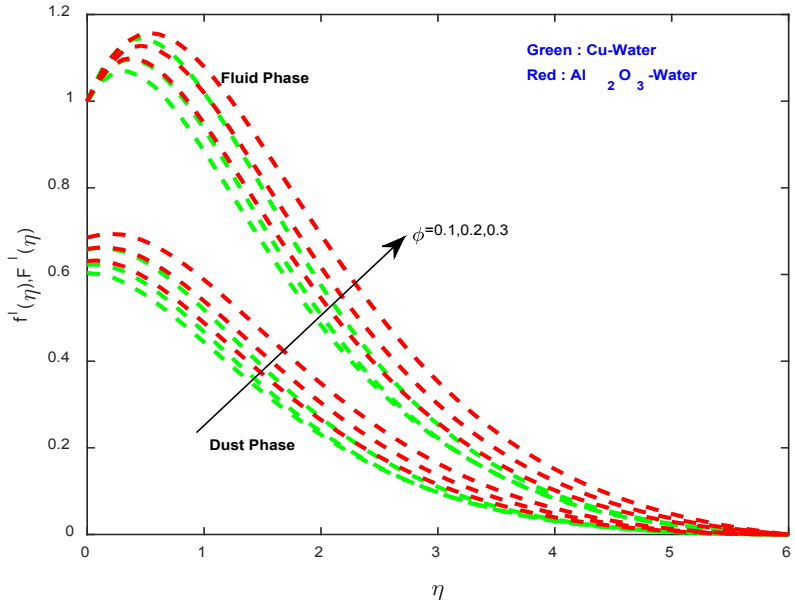

Figure 3 Velocity profiles for different values of volume fraction of nanoparticles ϕ .

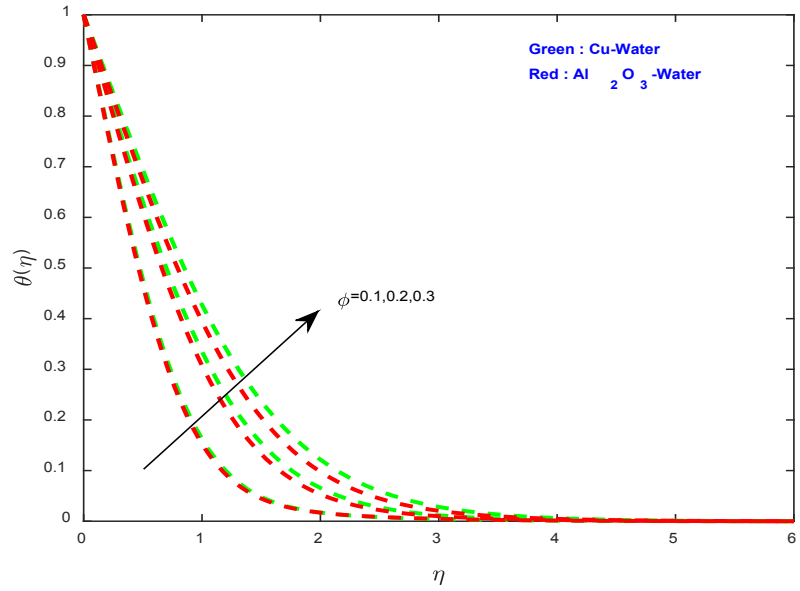

Figure 4 Temperature profiles for different values of volume fraction of nanoparticles ϕ .

Figure 5 depicts the velocity profiles of the fluid and dust phases for different values of volume fraction of dust particles ϕ_d . It is noticed that an increase in the volume fraction of dust particles reduces the velocity profiles of both fluid and dust phases. The reason behind this is, if the volume occupied by the dust particles per unit volume of the fluid is higher than the dust concentration in the fluid, then it leads to depreciation in the velocity boundary layer thickness.

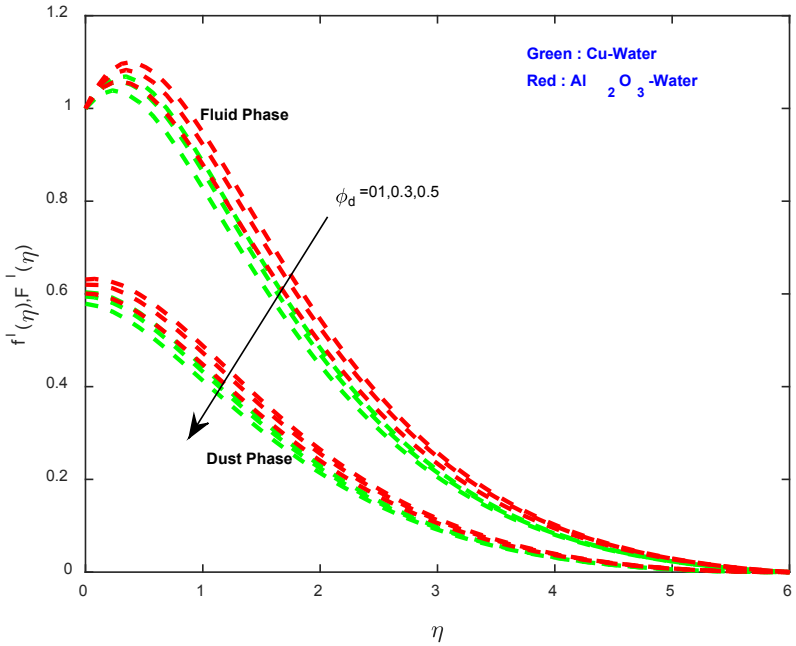

Figure 5 Velocity profiles for different values of volume fraction of dust particles ϕ_d.

The effect of mass concentration of dust particles α on velocity, temperature, and concentration profiles can be seen from **Figures 6 - 8**. It is observed that the velocity profiles of the fluid and dust phases are reduced with an enhancement in α , but we noticed the opposite results in temperature and concentration boundary layers. **Figure 9** depicts the velocity profiles of the fluid and dust phases for different values of fluid-particle interaction parameter β . We have observed an interesting result where an increase in the fluid-particle interaction parameter enhances the velocity of the dust phase, but depreciates the velocity of the fluid phase. This may happen due to the fact that, where the interaction between the fluid and particle phase is high, then the particle phase develops the opposite force to the fluid phase.

Figure 10 shows the effect of space dependent non-uniform heat source/sink parameter A^* on temperature profiles. It is evident that increase in A^* causes an increase in the temperature field. The reason behind this is that the thermal boundary layer generates the energy for positive values of A^* ; that is, positive values act like heat generators. The effect of buoyancy parameter on the velocity and concentration profiles is represented in **Figures 11** and **12** respectively. It is interesting to notice that an increase in the buoyancy parameter significantly enhances the velocity profiles of the fluid and dust phases. This helps to depreciate the concentration profiles.

Figures 13 and **14** display the influence of chemical reaction parameter on velocity and concentration profiles. It is clear that both velocity and concentration profiles decrease with an increase in the chemical reaction parameter. This agrees with the general physics behavior of the chemical reaction

parameter. It can be seen from **Table 2** that an enhancement in the physical parameters M, ϕ_d, α, β depreciates the profiles of the skin-friction coefficient and the Nusselt and Sherwood numbers, but the parameter λ helps to enhance the heat and mass transfer rate. **Table 3** shows the validation of the present results with the published work under some special limited cases. We observed good accuracy of the present results with the existing results. This proves that the present results are valid.

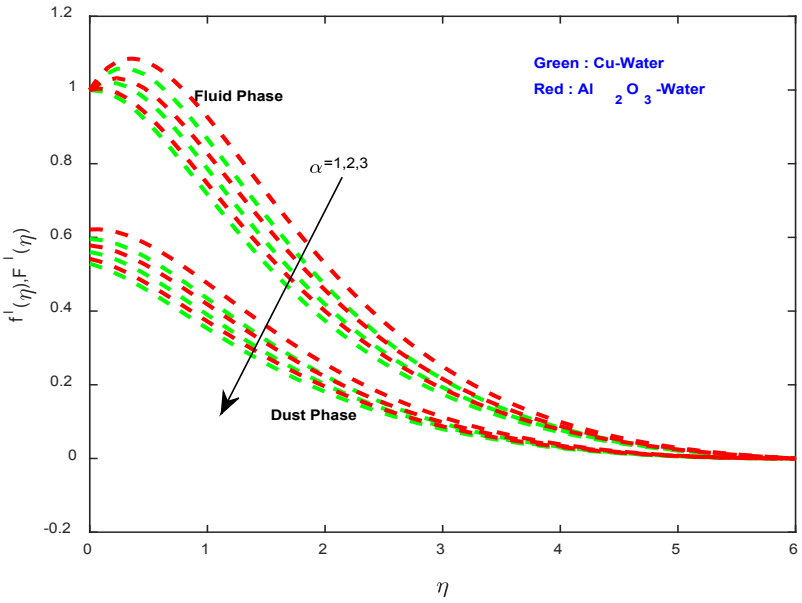

Figure 6 Velocity profiles for different values of mass concentration of dust particles α.

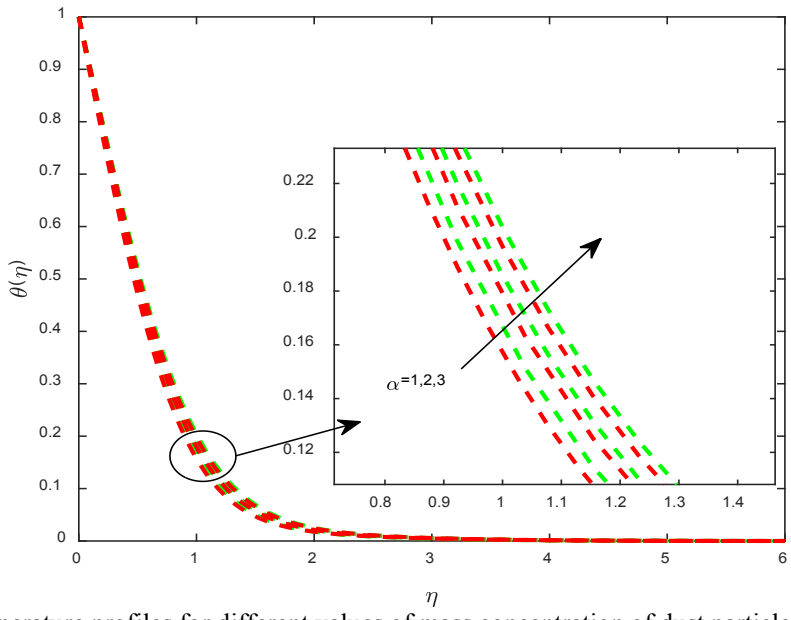

Figure 7 Temperature profiles for different values of mass concentration of dust particles α.

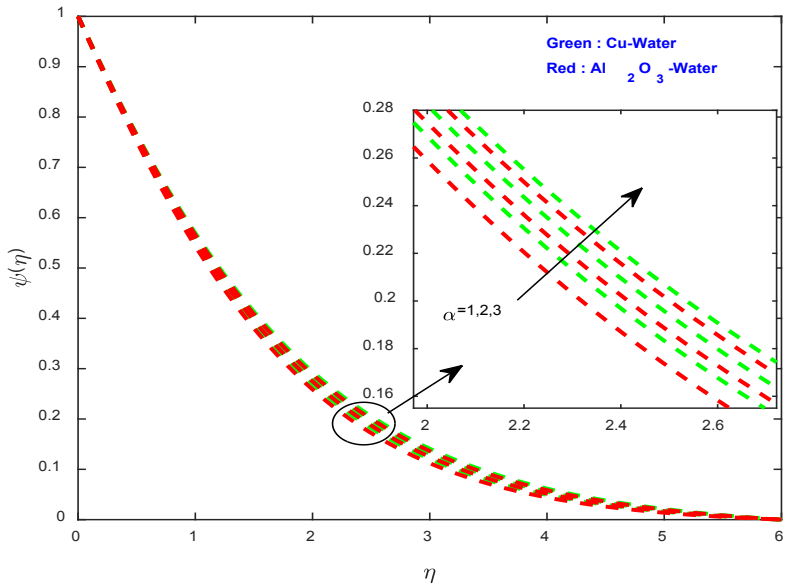

Figure 8 Concentration profiles for different values of mass concentration of dust particles α.

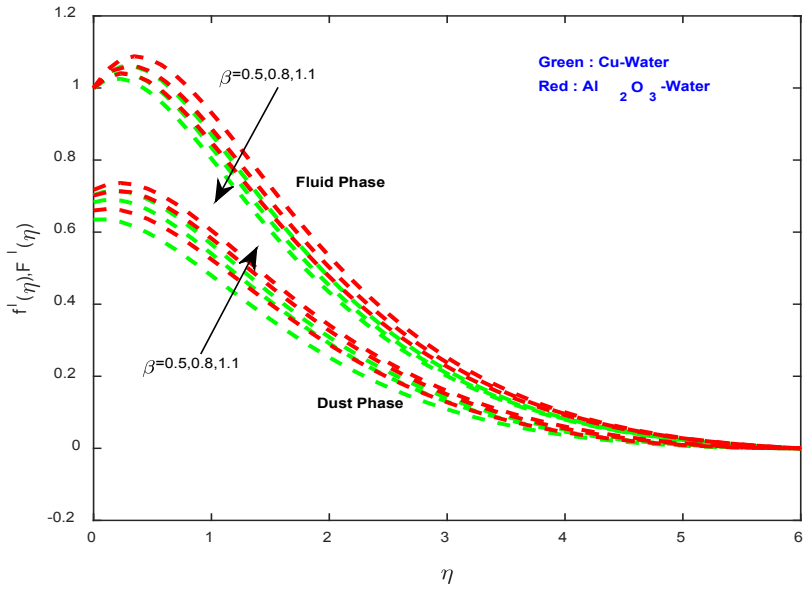

Figure 9 Velocity profiles for different values of fluid-particle interaction parameter β .

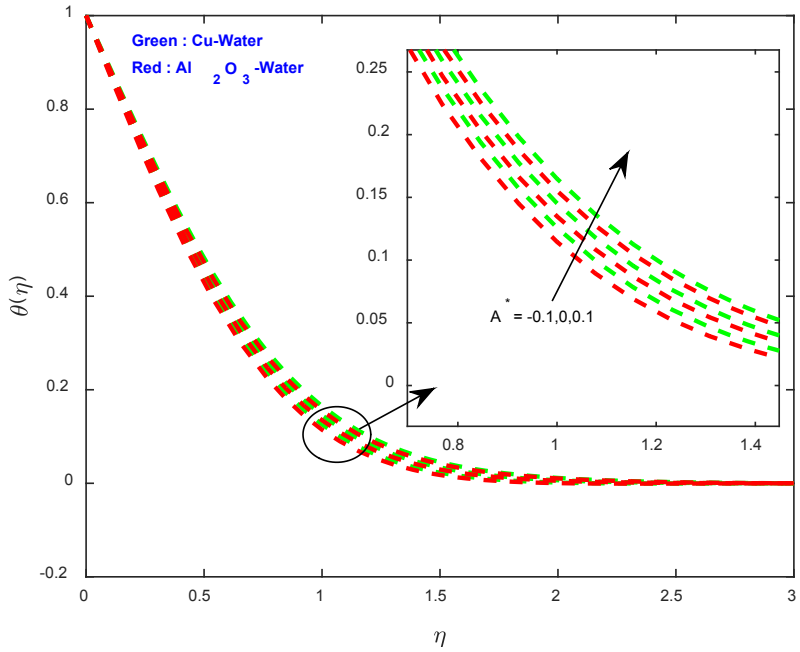

Figure 10 Temperature profiles for different values of non-uniform heat source/sink parameter A^*.

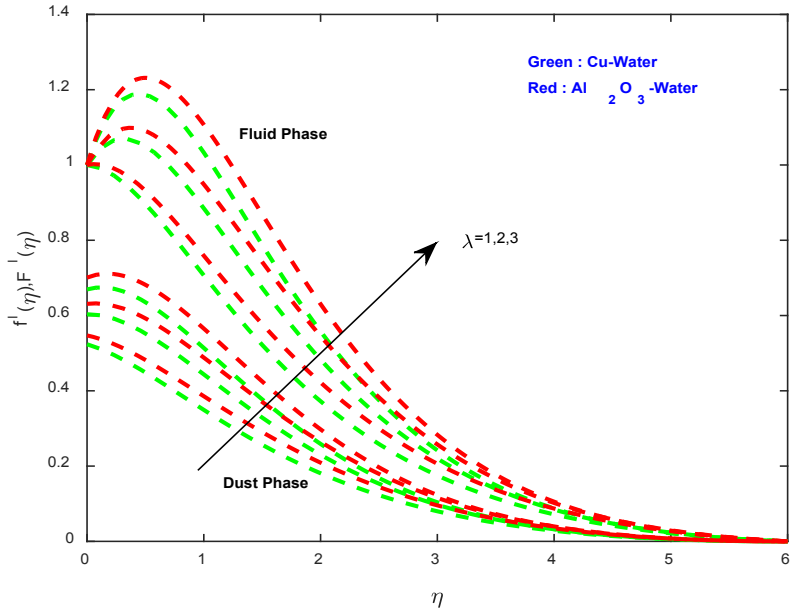

Figure 11 Velocity profiles for different values of buoyancy ratio parameter λ.

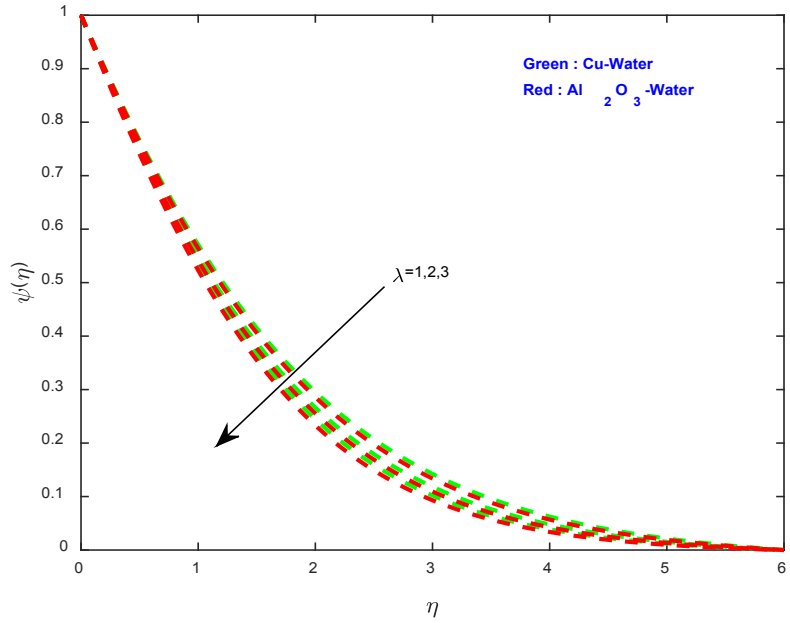

Figure 12 Concentration profiles for different values of buoyancy ratio parameter λ .

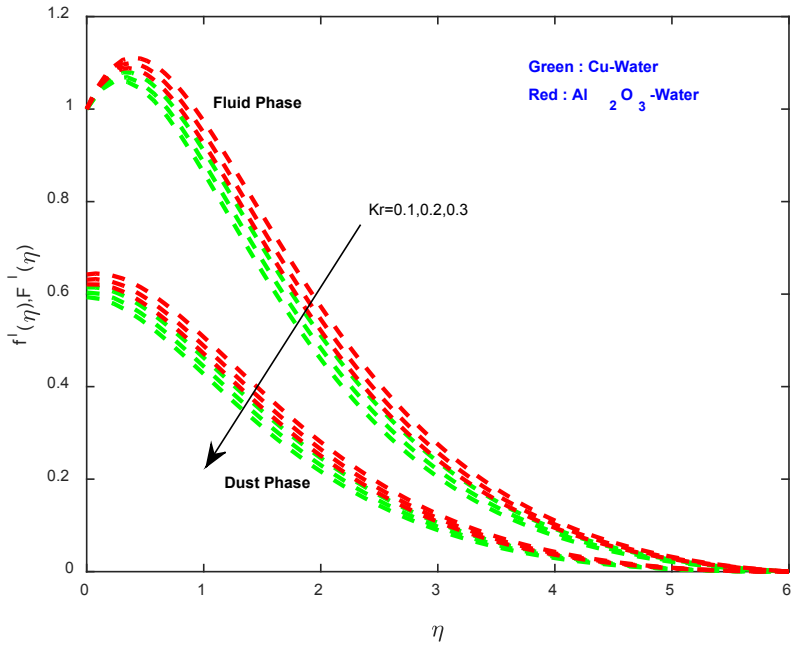

Figure 13 Velocity profiles for different values of chemical reaction parameter Kr .

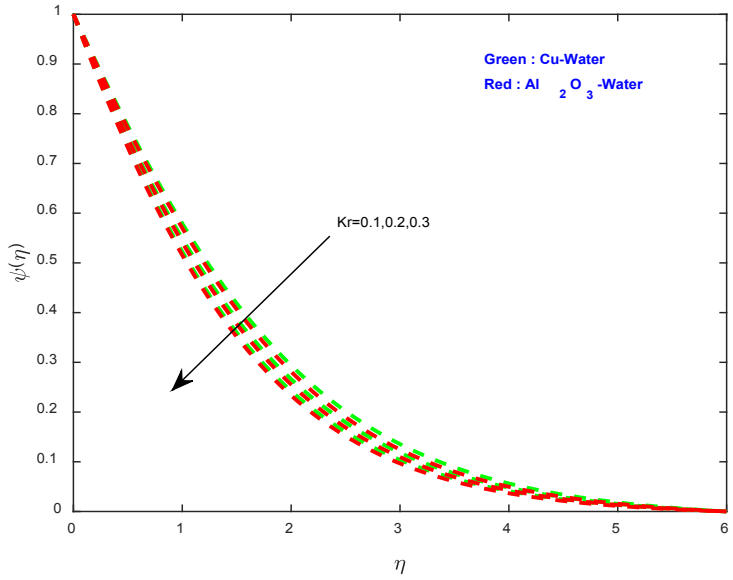

Figure 14 Concentration profiles for different values of chemical reaction parameter Kr .

Table 2 Variation in friction factor and local Nusselt and Sherwood numbers.

M	ϕ	ϕ_d	α	β	A^*	λ	Kr	$Cu-water$			$Al_2O_3-water$		
								C_f	Nu_x	Sh_x	C_f	Nu_x	Sh_x
1								0.3997	1.1037	0.5202	0.4809	1.1284	0.5275
2								0.2298	1.0837	0.5116	0.2922	1.1061	0.5170
3								0.0735	1.0647	0.5038	0.1218	1.0852	0.5079
	0.1							0.4093	1.1141	0.5249	0.5832	1.1401	0.5333
	0.2							0.5664	0.7513	0.5308	0.6157	0.7956	0.5416
	0.3							0.7029	0.6146	0.5412	0.6563	0.6599	0.5491
		0.1						0.4903	1.1141	0.5249	0.5832	1.1401	0.5333
		0.3						0.4395	1.1082	0.5222	0.5264	1.1335	0.5299
		0.5						0.3504	1.0978	0.5175	0.4276	1.1219	0.5242
			1					0.4469	1.1016	0.5226	0.5346	1.1268	0.5304
			2					0.2396	1.0426	0.5118	0.3057	1.0641	0.5174
			3					0.0470	0.9882	0.5022	0.0965	1.0069	0.5062
				0.5				0.4562	1.1096	0.5231	0.5451	1.1353	0.5311
				0.8				0.3620	1.0982	0.5184	0.4407	1.1229	0.5253
				1.1				0.2758	1.0880	0.5142	0.3457	1.1117	0.5203
					-			0.3716	1.2290	0.5636	0.4540	1.2600	0.5682
					0.0			0.3816	1.1646	0.5640	0.4647	1.1930	0.5687
					0.1			0.3916	1.0998	0.5645	0.4754	1.1255	0.5691
						1		0.20206	1.0558	0.5006	0.0711	1.0825	0.5079
						2		0.4903	1.1141	0.5249	0.5832	1.1401	0.5333
						3		0.9653	1.1592	0.5445	1.0588	1.1847	0.5536
							0.1	0.5240	1.1192	0.4686	0.6171	1.1450	0.4785
							0.2	0.4903	1.1141	0.5249	0.5832	1.1401	0.5333
							0.3	0.4603	1.1095	0.5768	0.5528	1.1357	0.5839

Table 3 Validation of the present study for $-\theta'(0)$ when $\beta = \beta_T = Ec = \phi_p = \phi = 0,$ $Sc = Kr = A^* = B^* = 0.$

Pr	Gireesha *et al*. [8]	Present study
0.72	1.0886	1.08857
1	1.3333	1.33333
10	4.7968	4.79681

Conclusions

This paper presents the momentum, heat, and mass transfer behaviour of chemically reacting MHD nanofluid flow embedded with the conducting dust particles past a cone in the presence of non-uniform heat source/sink, volume fractions of dust, and nanoparticles. The conclusions of the present study are as follows:

- The magnetic field parameter has the tendency to control the momentum boundary layer.
- Increase in the fluid particle interaction parameter increases the heat transfer rate.
- Increasing values of chemical reaction parameter enhances the mass transfer rate.
- An increase in the volume fraction of nanoparticles enhances the thermal conductivity of the flow.
- Rise in the volume fraction of dust particles reduces the momentum boundary layer thickness.
- Cu-water dusty nanofluid has better heat transfer performance when compared with Al_2O_3-water dusty nanofluid.

References

[1] H Masuda, A Ebata, K Teramae and N Hishinuma. Alteration of thermal conductivity and viscosity of liquid by dispersing ultra-fine particles. *Nets. Buss.* 1993; **7**, 227-33.
[2] MS Liu, MC Chang Len, IT Huang and CC Wang. Enhancement of thermal conductivity with carbon nanotube for nanofluids. *Int. Comm. Heat Mass Trans.* 2005; **32**, 1202-10.
[3] W Yu, H Xie, L Chen and Y Li. Enhancement of thermal conductivity of kerosene-based Fe_3O_4 nanofluids via phase- transfer method. *Coll. Surf. A: Physico. Eng. Asp.* 2010; **355**, 109-13.
[4] MP Beck, Y Yuan, P Warrier and AS Teja. The effect of particle size on the thermal conductivity of alumina nanofluid. *J. Nanopart. Res*. 2009; **11**, 1129-36.
[5] FG Awad, P Sibanda and AA Khidir. Thermo diffusion effects on magneto-nanofluid flow over a stretching sheet. *Bound. Val. Prob.* 2013; **136**, 1-13.
[6] CSK Raju, N Sandeep, C Sulochana, V Sugunamma and M Jayachandra Babu. Radiation, inclined magnetic field and cross diffusion effects on flow over a stretching surface. *J. Nig. Math. Soc*. 2015; **34**, 169-80.
[7] JV Ramana Reddy, V Sugunamma, P Mohan Krishna and N Sandeep. Aligned magnetic field, radiation and chemical reaction effects on unsteady dusty viscous flow with heat generation/ absorption. *Chem. Proc. Eng. Res*. 2014; **27**, 37-53.
[8] BJ Gireesha, GS Roopa, HJ Lokesh and CS Bajewadi. MHD flow and heat transfer of a dusty fluid over a stretching sheet. *Int. J. Phys. Math. Sci.* 2012; **3**, 171-82.
[9] N Sandeep and V Sugunamma. Radiation and inclined magnetic field effects on unsteady hydro magnetic free convection flow past an impulsively moving vertical plate in a porous medium. *J. Appl. Fluid Mech.* 2014; **7**, 275-86.
[10] GS Seth, R Sharma and S Sarkar. Natural convection heat and mass transfer flow with hall current, rotation radiation and heat absorption past an accelerated moving vertical plate with ramped temperature. *J. Appl. Fluid Mech*. 2015; **8**, 7-20.

[11] P Mohan Krishna, N Sandeep and V Sugunamma. Effects of radiation and chemical reaction on MHD convective flow over a permeable stretching surface with suction and heat generation. *Walailak. J. Sci. & Tech*. 2015; **12**, 831-47.
[12] NA Abu Bakar, K Zaimi and RA Hamid. MHD boundary layer flow of a Maxwell nanofluid over a permeable vertical surface. *AIP Conf. Proc.* 2014; **1605**, 422-7.
[13] K Vajravelu, KV Prasad, J Lee, C Lee, I Pop and RA Van Gorder. Convective heat transfer in the flow of viscous Ag-water and Cu-water nanofluids over a stretching surface. *Int. J. Therm. Sci.* 2011; **50**, 843-51.
[14] T Hayat, S Asad and A Alsaedi. Analysis for flow of Jeffrey fluid with nanoparticles. *Chin. Phys. B*. 2015; **24**, 044702.
[15] S Roy, P Datta, R Ravindran and E Momoniat. Non-uniform double slot injection (suction) on a forced flow over a slender cylinder. *Int. J. Heat Mass Tran.* 2007; **50**, 3190-94.
[16] R Ravindran, M Ganapathi Rao and I Pop. Effects of chemical reaction and heat generation/absorption on unsteady mixed convection MHD flow over a vertical cone with non-uniform slot mass transfer. *Int. J. Heat Mass Tran.* 2014; **73**, 743-51.
[17] NA Khan and F Sultan. On the double diffusive convection flow of eyring-powell fluid due to cone through a porous medium with soret and dufour effects. *AIP Adv.* 2015; **5**, 057140.
[18] M Awais, T Hayat, S Irum and A Alsedi. Heat generation/absorption effects in a boundary layer stretched flow of maxwell nanofluid: Analytic and numeric solutions. *PloS One* 2015; **10**, e0129814.
[19] T Hayat, T Hussain, SA Shehzad and A Alsaedi. Flow of Oldroid B-fluid with nano particles and thermal radiation. *Appl. Math. Mech.* 2015; **36**, 69-90.
[20] S Nadeem and S Saleem. Series solution of unsteady Eyring powell nanofluid flow on a rotating cone. *Ind. J. Pure Appl. Phys.* 2014; **52**, 725-37.
[21] B Vasu and K Manish. Transient boundary layer laminar free convective flow of a nanofluid over a vertical cone/plate. *Ind. J. Appl. Comput. Math.* 2015; **1**, 427-48.
[22] GK Ramesh. Numerical study of the influence of heat source on stagnation point flow towards a stretching surface of a jeffery nanoliquid. *J. Eng.* 2015; **2015**, 382061.
[23] RSR Gorla, BJ Gireesha and B Singh. MHD flow and heat transfer of dusty nanofluid embedded in porous medium over an exponentially stretching sheet. *J. Nanofluids* 2015; **4**, 1-12.
[24] N Sandeep and C Sulochana. MHD flow of dusty nanofluid over a stretching surface with volume fraction of dust particles. *Ain Shams Eng. J.* 2016; **7**, 709-16.
[25] D Pal. Combined effects of non-uniform heat source/sink and thermal radiation on heat transfer over an unsteady stretching permeable surface. *Commun. Nonlinear Sci. Numer. Simulat.* 2011; **16**, 1890-904.
[26] K Das. Flow and heat transfer characteristics of a nanofluids in a rotating frame. *Alex. Eng. J.* 2014; **53**, 757-66.
[27] B Mallikarjuna, AM Rashad, AJ Chamka and SHP Raju. Chemical reaction effects on MHD convective heat and mass transfer flow past a rotating vertical cone embedded in a variable porosity regime. *Afr. Mat.* 2016; **27**, 645-65.